Annals of Work Exposures and Health, 2024, **68**, 78–85
https://doi.org/10.1093/annweh/wxad064
Advance access publication 3 November 2023
Original Article

A decoupling method to compute near field and far field exposure concentrations

Mark Nicas*

School of Public Health, Environmental Health Sciences Division, 2121 Berkeley Way, University of California, Berkeley, CA 94740-7360, United States

*Corresponding author: School of Public Health, Environmental Health Sciences Division, 2121 Berkeley Way, University of California, Berkeley, CA 94740-7360, USA. Email: mnicas@berkeley.edu

Abstract

In the near field/far field (NF/FF) dispersion construct, the analytical solutions for the NF and FF concentration equations, respectively denoted $C_{NF}(t)$ and $C_{FF}(t)$ in mg/m^3, are coupled in their mathematical derivation. Depending on the form of the contaminant emission rate function $G(t)$ (mg/min), deriving $C_{NF}(t)$ and $C_{FF}(t)$ can range from being relatively easy to impossible. A method is presented to more easily approximate these concentration functions. The method decouples the NF and FF equations by treating the NF as an isolated well-mixed space with volume V_{NF} (m^3) and supply/exhaust airflow rate β(m^3) and treating the FF as an isolated well mixed-space with volume V (m^3) and supply/exhaust airflow rate Q (m^3). Assuming that each space contains a source with the same contaminant emission rate function $G(t)$, a contaminant concentration function is derived for the FF zone, denoted $C_{WMR1}(t)$, and an independent contaminant concentration function is derived for the NF zone, denoted $C_{WMR2}(t)$. Deriving a concentration function for a single zone is far easier than deriving coupled concentration functions. It is shown that the sum $C_{WMR1}(t) + C_{WMR2}(t)$ provides an excellent approximation of $C_{NF}(t)$ and that $C_{WMR1}(t)$ provides an excellent approximation of $C_{FF}(t)$. A discrete-time numerical solution for the $C_{NF}(t)$ and $C_{FF}(t)$ system based on a Markov matrix is also presented.

Key words: decoupling method; deterministic models; Markov matrix solution; near field/far field model; variable emission rates.

What's Important About This Paper?

The Near Field/Far Field model is widely used to estimate contaminant concentrations in workplaces, but prior solutions have utilized relatively simple emission functions. This study presents a method that facilitates the application of the Near Field/Far Field model where it is mathematically difficult to derive the coupled time-dependent contaminant concentration functions.

Introduction

The near field/far field (NF/FF) model is a contaminant-in-air dispersion construct widely used in the industrial hygiene profession (IH MOD 2.0 2023). It has been shown that the model usually provides NF contaminant exposure estimates within a 2-fold factor of the corresponding measured concentrations (Jayjock et al. 2011). In accounting for higher exposure intensity near an emission source, the model also maintains a contaminant mass balance within the room, unlike the well-mixed room model employing a mixing factor (ACGIH 1998), and unlike the commonly used versions of turbulent diffusion models (Nicas 2009). The conceptual framework for the NF/FF model was first presented in a ventilation text about seven decades ago (Hemeon 1955); the time-dependent concentration equations given a constant contaminant emission rate were derived and published 4 decades later (Nicas 1996).

Received: August 6, 2023. Accepted: October 12, 2023.

The NF/FF model is not limited to considering only constant emission, for which the rate is usually denoted G (mg/min), but extends to continuous time-varying emission rate functions which can be denoted $G(t)$. The most frequently applied $G(t)$ function is an exponentially decreasing emission rate:

$$G(t) = \alpha \times M_0 \times \mathbf{exp}(-\alpha \times t) \quad (1)$$

where (i) M_0 is the contaminant mass (mg) in the source at time t (min) equal to zero, (ii) no further contaminant mass is added to the source, and (iii) α is a first-order loss rate constant with unit min^{-1} (Keil and Nicas 2003).

A second published $G(t)$ function involves exponentially decreasing emission from material that is applied to a surface at a constant rate per Equation 2 below:

$$G(t) = I \times [1 - \mathbf{exp}(-\alpha \times t)] \quad (2)$$

where (i) I is the constant mass rate (mg/min) of contaminant added to the surface and (ii) α is the same parameter as in Equation (1) (Nicas 2016).

A third published $G(t)$ function involves cyclical (sinusoidal) emission per Equation 3 below:

$$G(t) = \frac{G_{\mathbf{max}}}{2} \times \left[\mathbf{sin}\left(\frac{2\pi}{t_{\mathbf{cycle}}} \times t - \frac{\pi}{2}\right) + \mathbf{1}\right] \quad (3)$$

where (i) G_{max} (mg/min) is the maximum emission rate, and (ii) t_{cycle} (min) is the time to complete 1 cycle (period) of emission (Nicas and Armstrong 2003).

Analytical solutions for the NF/FF model have been published based on assuming the NF zone emission source has, alternatively: (i) a constant emission rate, (ii) an exponentially decreasing emission rate, and (iii) exponentially decreasing emission from material constantly being applied to the surface. An analytical solution means there are closed-form equations for the coupled time-dependent contaminant concentration functions in the NF zone, denoted $C_{NF}(t)$ in mg/m^3, and in the FF zone, denoted $C_{FF}(t)$ in mg/m^3. An analytical solution is not yet available for the NF/FF model with a sinusoidal emission rate from the NF zone, but a numerical solution will be presented.

Depending on the nature of the $G(t)$ function, deriving coupled solutions analytically for $C_{NF}(t)$ and $C_{FF}(t)$ can range from tedious to impossible, and a numerical solution can involve computer implementation that is much more complicated than feasibly performed via a spreadsheet. In turn, difficulty in analytically or numerically formulating the coupled solutions can limit the application of the NF/FF model to only mathematically "convenient" $G(t)$ functions which may not be adequate descriptors. This article shows that excellent approximations for $C_{NF}(t)$ and $C_{FF}(t)$ can be more simply derived based on two decoupled well-mixed space constructs. An explanation of the method is now presented based on a constant contaminant emission rate.

The decoupling method for a constant emission rate

In the NF/FF model with a constant emission rate G, the NF steady-state concentration C_{NFSS} equals the sum $G/\beta + G/Q$, and the FF steady-state concentration C_{FFSS} equals G/Q, where β is the volumetric airflow rate (m^3/min) into and out of the NF zone, and Q is the volumetric airflow rate (m^3/min) into and out of the room. For C_{NFSS}, the quantity G/β is the concentration component due to direct contaminant emission into the NF zone, and the quantity G/Q is the concentration component due to FF zone air carried back into the NF zone. This circumstance suggests that the $C_{NF}(t)$ can be approximated as the sum of 2 non-linked time-dependent concentration equations. The first is labeled $C_{WMR1}(t)$ and is the traditional well-mixed room equation with parameters Q and V (m^3, the room volume):

$$C_{\mathbf{WMR1}}(t) = \frac{G}{Q} \times \left[\mathbf{1} - \mathbf{exp}\left(-\frac{Q}{V} \times t\right)\right] \quad (4)$$

For simplicity, it is assumed $C_{WMR1}(0) = 0$. It will be shown that $C_{WMR1}(t)$ is an excellent approximation of the analytically-derived $C_{FF}(t)$ equation; the approximation is denoted $C_{FF}{}^*(t)$

$$C_{\mathbf{FF}}(t) \cong C_{\mathbf{FF}*}(t) = C_{\mathbf{WMR1}}(t) \quad (5)$$

The second equation is labeled $C_{WMR2}(t)$ and treats the NF zone as an isolated well-mixed space with parameters β and V_{NF} (m^3, the NF volume), where $C_{WMR2}(0) = 0$:

$$C_{\mathbf{WMR2}}(t) = \frac{G}{\beta} \times \left[\mathbf{1} - \mathbf{exp}\left(-\frac{\beta}{V_{\mathbf{NF}}} \times t\right)\right] \quad (6)$$

The analytically-derived $C_{NF}(t)$ equation is approximated by the sum of $C_{WMR1}(t)$ and $C_{WMR2}(t)$, denoted $C_{NF}{}^*(t)$:

$$C_{\mathbf{NF}}(t) \cong C_{\mathbf{NF}*}(t) = C_{\mathbf{WMR1}}(t) + C_{\mathbf{WMR2}}(t) \quad (7)$$

Whereas analytically deriving $C_{NF}(t)$ and $C_{FF}(t)$ requires solving 2 coupled differential equations (Nicas 1996) deriving either $C_{WMR1}(t)$ or $C_{WMR2}(t)$ involves solving 1 differential equation. If one solves for $C_{WMR1}(t)$, the parameters Q and V can simply be replaced by the respective parameters β and V_{NF} to obtain $C_{WMR2}(t)$, and vice versa.

To illustrate the method, consider the following hypothetical scenario. The NF is a cube with length aspect 1 m that sits on a surface, such that $V_{NF} = 1\ m^3$ and the free surface area FSA = 5 m^2. The random air speed (denoted s) at the NF boundary is 4.6 m/min (or 15 fpm), such that $\beta = ½ \times FSA \times s = 11.5\ m^3$/min, and

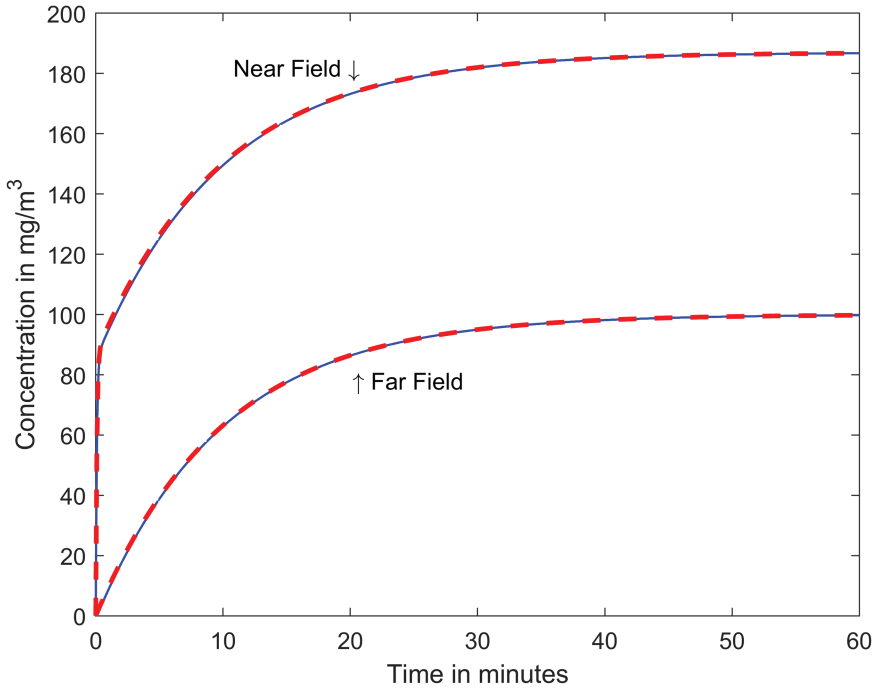

Fig. 1. The near field/far field model with a constant contaminant emission rate. $C_{NF}(t)$ is the solid-line curve and $C_{NF}^*(t)$ is the dashed-line curve corresponding to the "Near Field" arrow. $C_{FF}(t)$ is the solid-line curve and $C_{FF}^*(t)$ is the dashed-line curve corresponding to the "Far Field" arrow.

$\beta / V_{NF} = 11.5$ min^{-1}. The room has $V = 100$ m^3 and $Q = 10$ m^3/min, such that $Q/V = 0.1$ min^{-1}. Let $G = 1{,}000$ mg/min. The corresponding approximation equations for $t \geq 0$ min are as follows:

$$C_{WMR1}(t), \mathbf{mg/m^3} = \mathbf{100} \times [\,1 - \mathbf{exp}(-\mathbf{0.1} \times t)] \quad (8a)$$

$$C_{WMR2}(t), \mathbf{mg/m^3} = \mathbf{87} \times [1 - \mathbf{exp}(-\mathbf{11.5} \times t)] \quad (8b)$$

$$C_{FF*}(t), \mathbf{mg/m^3} = \mathbf{100} \times [1 - \mathbf{exp}(-\mathbf{0.1} \times t)] \quad (8c)$$

$$C_{NF*}(t), \mathbf{mg/m^3} = 100 \times [1 - \mathbf{exp}(-\mathbf{0.1} \times t)] + 87 \times [1 - \mathbf{exp}(-\mathbf{11.5} \times t)] \quad (8d)$$

The general solution equations for $C_{NF}(t)$ and $C_{FF}(t)$ have been published previously (Nicas 1996). The specific equations for the present scenario are as follows:

$$C_{NF}(t), \mathbf{mg/m^3} = -\mathbf{101.8} \times \exp(-\mathbf{0.10} \times t) - \mathbf{85.2} \times \exp(-\mathbf{11.62} \times t) + \mathbf{187} \quad (9a)$$

$$C_{FF}(t), \mathbf{mg/m^3} = -\mathbf{100.9} \times \exp(-\mathbf{0.10} \times t) + \mathbf{0.9} \times \exp(-\mathbf{11.62} \times t) + \mathbf{100} \quad (9b)$$

Figure 1 graphs $C_{NF}(t)$ (the solid-line curve) versus its approximation $C_{NF}^*(t)$ (the dashed-line curve), which are both labeled "Near Field," over a 1-h period. Figure 1 also graphs $C_{FF}(t)$ (the solid-line curve) versus its approximation $C_{FF}^*(t)$ (the dashed-line curve), which are both labeled "Far Field," over a 1-h period. The curves for the approximate and analytical solutions are nearly coincident. The maximum difference between $C_{NF}^*(t)$ and $C_{NF}(t)$ is 1.7 mg/m^3 (only 0.9% of the 187 mg/m^3 steady-state C_{NF} value), and the maximum difference between $C_{FF}^*(t)$ and $C_{FF}(t)$ is 0.88 mg/m^3 (only 0.9% of the 100 mg/m^3 steady-state C_{FF} value).

The decoupling method for an exponentially decreasing emission rate

In the NF/FF model with a $G(t)$ function per Equation 1, a steady-state concentration does not evolve. In either zone, the contaminant concentration increases to a peak value and subsequently declines to zero. Where $C_{WMR1}(0) = 0$, the $C_{WMR1}(t)$ equation is as follows:

$$C_{WMR1}(t) = \frac{\alpha \times M_0}{\alpha \times V - Q} \times \left[\mathbf{exp}\left(-\frac{Q}{V} \times t\right) - \mathbf{exp}(-\alpha \times t)\right] \quad (10)$$

For space considerations, the $C_{WMR2}(t)$ equation is not shown, but it replaces Q with β and replaces V with V_{NF}. As before, $C_{NF}^*(t) = C_{WMR1}(t) + C_{WMR2}(t)$.

To demonstrate the method's performance, consider a similar hypothetical scenario. The NF is a cube with a length aspect of 1 m that sits on a surface, such that V_{NF} = 1 m^3. The random air speed at the NF boundary is 4.6 m/min such that β = 11.5 m^3/min. The room has V = 100 m^3 and Q = 10 m^3/min. In this case, let M_0 = 63 200 mg and α = 0.05 min^{-1}, such that in 1 h about 60 000 mg of contaminant are emitted from the source, the same mass emitted into room air during a 1-h period in the previous constant emission rate scenario. The corresponding approximation equations for $t \geq 0$ min are as follows:

$$C_{WMR1}(t), \mathbf{mg/m^3} = -\mathbf{632} \times [\exp(-\mathbf{0.1} \times t) - \exp(-\mathbf{.05} \times t)] \quad (11a)$$

$$C_{WMR2}(t), \mathbf{mg/m^3} = -\mathbf{276} \times [\exp(-\mathbf{11.5} \times t) - \exp(-\mathbf{.05} \times t)] \quad (11b)$$

In turn: $C_{NF}{}^*(t) = C_{WMR1}(t) + C_{WMR2}(t)$, and $C_{FF}{}^*(t) = C_{WMR1}(t)$.

The general solution equations for $C_{NF}(t)$ and $C_{FF}(t)$ have been published previously (Keil and Nicas 2003). The specific equations for this scenario are as follows:

$$C_{NF}(t), \mathbf{mg/m^3} = -\mathbf{643.1} \times \exp(-\mathbf{0.10} \times t) - \mathbf{270.4} \times \exp(-\mathbf{11.62} \times t) + \mathbf{913.5} \times \exp(-\mathbf{.05} \times t) \quad (12a)$$

$$C_{FF}(t), \mathbf{mg/m^3} = -\mathbf{637.5} \times \exp(-\mathbf{0.10} \times t) + \mathbf{2.7} \times \exp(-\mathbf{11.62} \times t) + \mathbf{634.8} \times \exp(-\mathbf{.05} \times t) \quad (12b)$$

Figure 2 graphs $C_{NF}(t)$ (the solid-line curve) versus its approximation $C_{NF}{}^*(t)$ (the dashed-line curve), which are both labeled "Near Field," over a 1-h period. Figure 2 also graphs $C_{FF}(t)$ (the solid-line curve) versus its approximation $C_{FF}{}^*(t)$ (the dashed-line curve), which are both labeled "Far Field," over a 1-h period. The curves for the approximate and analytical solutions are nearly coincident. The maximum difference between $C_{NF}{}^*(t)$ and $C_{NF}(t)$ is 5.2 mg/m^3 (only 1.6% of the 324 mg/m^3 peak $C_{NF}(t)$ value), and the maximum difference between $C_{FF}{}^*(t)$ and $C_{FF}(t)$ is 2.7 mg/m^3 (only 1.7% of the 157 mg/m^3 peak $C_{FF}(t)$ value).

It has been shown previously that the decoupling method provides an excellent approximation for $C_{NF}(t)$ and $C_{FF}(t)$ in the related scenario of exponentially decreasing emission from material applied to a surface at a constant rate per Equation 2 (Nicas 2016). Therefore, an example is not provided here.

The decoupling method for a sinusoidal emission rate

In the NF/FF model with a $G(t)$ function per Equation 3, a steady-state concentration per se does not evolve.

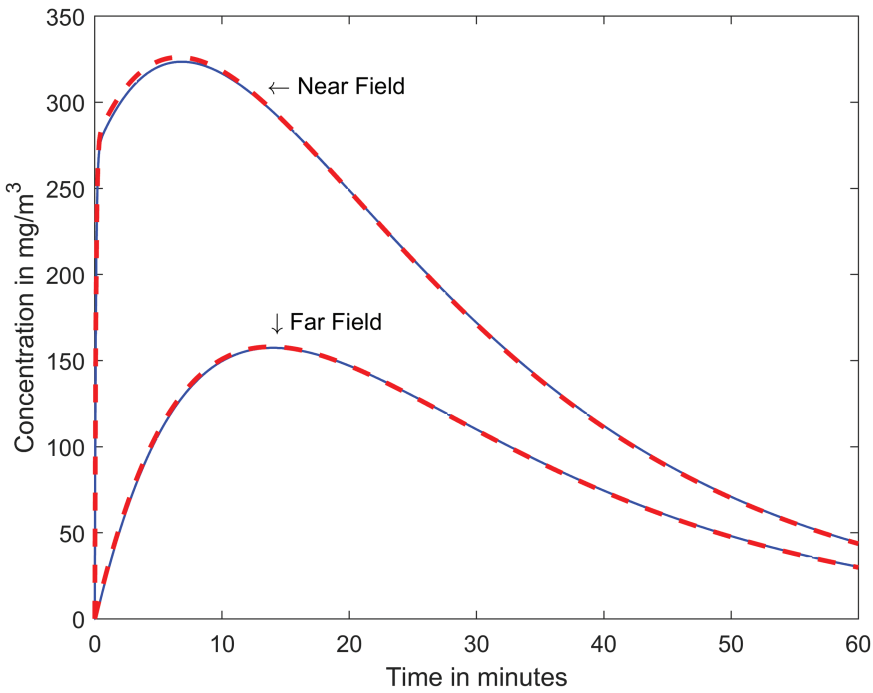

Fig. 2. The near field/far field model with an exponentially decreasing contaminant emission rate. $C_{NF}(t)$ is the solid-line curve and $C_{NF}{}^*(t)$ is the dashed-line curve corresponding to the "Near Field" arrow. $C_{FF}(t)$ is the solid-line curve and $C_{FF}{}^*(t)$ is the dashed-line curve corresponding to the "Far Field" arrow.

Instead, in either zone, the contaminant concentration attains a steady-state moving average such that the concentration increases and decreases in a sinusoidal fashion around a constant mean value. Where $C_{WMR1}(0) = 0$, the $C_{WMR1}(t)$ equation is as follows:

$$C_{WMR1}(t) = \frac{G_{max}}{2 \times Q} \times \left[1 - \exp\left(-\frac{Q}{V} \times t\right)\right] + \frac{G_{max} \times Q}{8\left(\frac{\pi \times V}{t_{cycle}}\right)^2 + 2 \times Q^2} \times \left[\exp\left(-\frac{Q}{V} \times t\right) + \sin\left(\frac{2\pi \times t}{t_{cycle}} - \frac{\pi}{2}\right) - \frac{2\pi \times V}{Q \times t_{cycle}} \times \cos\left(\frac{2\pi \times t}{t_{cycle}} - \frac{\pi}{2}\right)\right] \quad (13)$$

For space considerations, the $C_{WMR2}(t)$ equation is not shown, but it replaces Q with β and replaces V with V_{NF}. As before, $C_{NF}{}^*(t) = C_{WMR1}(t) + C_{WMR2}(t)$.

To demonstrate the decoupling method's performance, consider another hypothetical scenario. As before, the NF is a cube with a length aspect of 1 m that sits on a surface, such that $V_{NF} = 1\ m^3$. The random air speed at the NF boundary is 4.6 m/min such that $\beta = 11.5\ m^3/min$. The room has $V = 100\ m^3$ and $Q = 10\ m^3/min$. In this case, let $G_{max} = 2{,}000$ mg/min and $t_{cycle} = 10$ min, such that in 1 h 60 000 mg of contaminant are emitted from the source, which is the same total mass emitted in the previous scenarios. The corresponding approximation equations for $t \geq 0$ min are as follows:

$$C_{WMR1}(t), mg/m^3 = 100 \times [1 - \exp(-0.1 \times t)] + 2.471 \times \left[\exp(-0.1 \times t) + \sin\left(0.2\pi \times t - \frac{\pi}{2}\right) - 26.283 \times \cos\left(0.2\pi \times t - \frac{\pi}{2}\right)\right] \quad (14a)$$

$$C_{WMR2}(t), mg/m^3 = 86.957 \times [1 - \exp(-0.1 \times t)] + 86.698 \times \left[\exp(-0.1 \times t) + \sin\left(0.2\pi \times t - \frac{\pi}{2}\right) - .0546 \times \cos\left(0.2\pi \times t - \frac{\pi}{2}\right)\right] \quad (14b)$$

As before: $C_{NF}*(t) = C_{WMR1}(t) + C_{WMR2}(t)$, and $C_{FF}*(t) = C_{WMR1}(t)$

The numerical solutions for $C_{NF}(t)$ and $C_{FF}(t)$ are based on the first-order loss rates from the NF and FF zones, respectively, incorporated into a Markov matrix denoted $\boldsymbol{P}$ (Nicas, 2011). The $\boldsymbol{P}$ matrix is described in Appendix 1 of the Supplementary file. To briefly explain the numerical method, one poses a small-time interval, here $\Delta t = 0.0001$ min, and computes the mass emitted in each interval running from the first interval up through the last interval with an end time denoted t_{end}. For each interval, the mass that was emitted and is present at the time t_{end} in the respective NF and FF zone is computed; these remaining masses are summed and divided by the zone volume to yield the contaminant concentrations $C_{NF}(t_{end})$ and $C_{FF}(t_{end})$. The shorter the Δt value, the closer the discrete-time numerical method conforms to a continuous-time process. However, for Δt equal to 10^{-3} min versus 10^{-4} min, there is only a 0.5% difference in the 1-h TWA values for $C_{NF}(t)$.

The mass emitted in the interval t to $t + \Delta t$ is the definite integral of the Equation 3 function from t to $t + \Delta t$, as follows:

$$\text{Mass emitted in interval } [t, t+\Delta t] = \frac{G_{max}}{2} \times \left(\Delta t + \frac{t_{cycle}}{2\pi} \times \left\{\cos\left[\frac{2\pi}{t_{cycle}} \times t - \frac{\pi}{2}\right] - \cos\left[\frac{2\pi}{t_{cycle}} \quad (t+\Delta t) - \frac{\pi}{2}\right]\right\}\right) \quad (15)$$

The value of $C_{NF}(t_{end})$ is computed as follows:

$$C_{NF}(t_{end}) = \sum_{i=1}^{n} \frac{M_i}{V_{NF}} \times p_{11}^{ni+1} \quad (16)$$

where (i) $n = (t_{end}/\Delta t) \times 10^4$, (ii) M_i is the mass emitted in the ith interval, and (iii) p_{11}^{n-i+1} is the entry in the first row and first column of the $\boldsymbol{P}$ matrix multiplied by itself n–i+1 times. Note that p_{11}^{1} is the entry in the first row and first column of the $\boldsymbol{P}$ matrix.

Similarly, the value of $C_{FF}(t_{end})$ is computed as follows:

$$C_{FF}(t_{end}) = \sum_{i=1}^{n} \frac{M_i}{V} \times p_{12}^{n-i+1} \quad (17)$$

The terms n and M_i are the same as in Equation 16, and p_{12}^{n-i+1} is the entry in the first row and second column of the $\boldsymbol{P}$ matrix multiplied by itself n–i+1 times. p_{12}^{1} is the entry in the first row and second column of the $\boldsymbol{P}$ matrix.

Figure 3 graphs $C_{NF}(t)$ (the solid-line curve) versus its approximation $C_{NF}{}^*(t)$ (the dashed-line curve), which are both labeled "Near Field," over a 1-h period. Figure 3 also graphs $C_{FF}(t)$ (the solid-line curve) versus its approximation $C_{WMR1}(t)$ (the dashed-line curve), which are both labeled "Far Field," over a 1-h period. The curves for the approximate and numerical solutions are nearly coincidental. The maximum difference between $C_{NF}{}^*(t)$ and $C_{NF}(t)$ is 3.4 mg/m^3 (only 1.2% of the 276 mg/m^3 peak $C_{NF}(t)$ value), and the maximum difference between $C_{FF}{}^*(t)$ and $C_{FF}(t)$ is 1.7 mg/m^3 (only 1.5% of the 115 mg/m^3 peak $C_{FF}(t)$ value). The Matlab computer code used to find the $C_{NF}(t)$ and $C_{FF}(t)$ series is presented in Appendix 2 of the Supplementary file.

Discussion

Performance for different β and Q values

For a fixed NF volume, β determines how rapidly the contaminant emitted into the NF zone disperses into the FF zone, and for a fixed room volume, Q determines how rapidly the contaminant is exhausted from

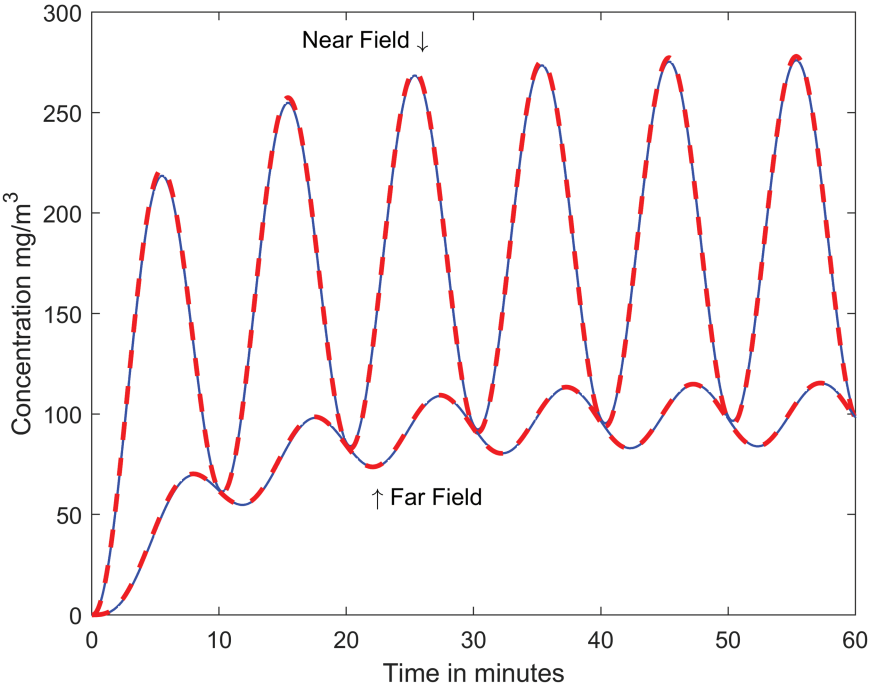

Fig. 3. The near field/far field model with a sinusoidal fluctuating emission rate. $C_{NF}(t)$ is the solid-line curve and $C_{NF}^*(t)$ is the dashed-line curve corresponding to the "Near Field" arrow. $C_{FF}(t)$ is the solid-line curve and $C_{FF}^*(t)$ is the dashed-line curve corresponding to the "Far Field" arrow.

the room. In the illustrative scenarios considered, β = 11.5 m^3/min corresponded to 11.5 air changes per minute (ACM) for V_{NF} = 1 m^3, and Q = 10 m^3/min corresponded to 0.1 ACM (or 6 ACH) for V = 100 m^3. The decoupling method worked well for this plausible pair of β and Q values, but does it also work for more extreme β and Q values?

To investigate the issue, four combinations of β and Q values were considered: (i) β = 1.5 m^3/min and Q = 0.83 m^3/min, (ii) β = 1.5 m^3/min and Q = 50 m^3/min, (iii) β = 50 m^3/min and Q = 0.83 m^3/min, and (iv) β = 50 m^3/min and Q = 50 m^3/min. For the cubic NF geometry that was posed, the β values of 1.5 and 50 m^3/min correspond to random air speeds of, respectively, 0.6 m/min (2 feet per minute, fpm) and 19.8 m/min (65 fpm). These 2 values are in the tails of the reported lognormal distribution of indoor air speeds with geometric mean = 3.6 m/min (11.8 fpm) and geometric SD = 1.96 (Baldwin and Maynard 1998). For room volume V = 100 m^3, the Q values of 0.83 and 50 m^3/min correspond to ACH values of, respectively, 0.5 and 30 h^{-1}, which are at the tails of the plausible range of air exchange values for industrial and commercial workplaces.

The constant emission rate, exponentially decreasing emission rate, and sinusoidal emission rate functions previously posed in the illustrative scenarios were considered with these β and Q combinations. Respective Supplementary Tables S1 to S3 in the supplementary file summarize the following output: (i) the 60-min TWA value computed by the coupled solution (denoted CS TWA), (ii) the average absolute difference between the coupled solution and the decoupled solution (denoted Diff. Av.) at 6 × 10^5 equidistant time points across the 60-min period, (iii) the maximum concentration computed by the coupled solution (denoted CS Max.), and (iv) the absolute difference between the respective maximum concentrations for the coupled and decoupled solutions over the 60-min period (denoted Diff. Max.). The tables also show the output for the illustrative scenario combination of β = 11.5 m^3/min and Q = 10 m^3/min.

For a constant emission rate and for both the NF and FF concentrations, the percentage differences between Diff. Av. and CS TWA, and the percentage differences between Diff. Max. and CS Max., are ≤1.2% across all β and Q combinations except for 1. For β = 1.5 m^3/min and Q = 0.83 m^3/min, the percentage difference between the FF CS Max. and Diff. Max. values is 2.1%.

For an exponentially decreasing emission rate and for both the NF and FF concentrations, the percentage differences between Diff. Av. and CS TWA, and the percentage differences between Diff. Max. and CS Max., are ≤2.1% across all β and Q combinations except for 1. For β = 1.5 m^3/min and Q = 50 m^3/min, the

percentage difference between the FF CS Max. and FF Diff. Max. values is 5.5%. However, focusing on the average *absolute* difference is a worst-case comparison, because the average difference (the mean of FF Diff. Max. minus FF CS Max.) for this β and Q combination corresponds to a 0.21% difference; in turn, the FF 60-min TWAs computed by the coupled and decoupled solutions differ by only 0.21%.

For a sinusoidal emission rate and for both the NF and FF concentrations, the percentage differences between Diff. Av. and CS TWA, and the percentage differences between Diff. Max. and CS Max., are ≤2.9% across all β and Q combinations except for 1. For β = 1.5 m^3/min and Q = 50 m^3/min, the percentage difference between the FF CS TWA and FF Diff. Av. values are 16%, and between the FF CS Max. and FF Diff. Max. values is 3.2%. Again, focusing on the average *absolute* difference is a worst-case comparison, because the average difference (the mean of FF Diff. Max. minus FF CS Max.) for this β and Q combination corresponds to a 1.0% difference; in turn, the FF 60-min TWAs computed by the coupled and decoupled solutions differ by only 1.0%. Part of the reason for the discrepancy can be seen in a graph (not shown) of the FF concentration time series for the coupled and decoupled solutions. The sinusoidal peaks (and troughs) occur about half a minute earlier for the decoupled solution, which causes the mean absolute difference to be greater than the mean differences across the time points. The offset occurs because the decoupled solution is based on the instantaneous emission of a contaminant into the FF zone, whereas β = 1.5 m^3/min (or 1.5 ACM) in the coupled solution involves a slower release into the FF zone.

Other considerations

The model equations discussed here apply to gas-phase contaminants and, in general, not to particulate contaminants. The reason is that the loss rate constants accounted for only exhaust air flows (β and Q) and not for particle loss by gravitational settling and deposition onto vertical surfaces in the NF and FF zones. Given the same mass of contaminant emitted into NF zone air, the particle loss pathways would decrease particulate contaminant concentrations relative to those for a gas-phase contaminant. Particle loss rates can also be posed as first-order rates with an inverse time unit, but their values depend on particle aerodynamic diameter. A further complication is that particulate contaminants are almost always emitted as a distribution of aerodynamic particle sizes, so one needs to consider a distribution of loss rates.

The decoupling method $C_{NF}{}^*(t)$ approximation is based on a superposition principle, that is, the solution is the sum of 2 independent equations. The equations $C_{WMR1}(t)$ and $C_{WMR2}(t)$ are independent in that neither depends on the other. A superposition principle also applies to the $C_{FF}{}^*(t)$ approximation where there are 2 or more emission sources in the room. To explain, consider 2 NF zones in a room, where NF #1 contains a source with an emission rate of $G_1(t)$, and NF #2 contains a source with a different emission rate of $G_2(t)$. The 2 sources generate the respective room concentration series $C_{WMR1–G1}(t)$ and $C_{WMR1–G2}(t)$, where the G_1 and G_2 subscripts index the sources. In this situation: $C_{FF}{}^*(t) = C_{WMR1–G1}(t) + C_{WMR1–G2}(t)$, but the respective $C_{WMR2}(t)$ equations for the 2 NF zones are not affected. Where there are 2 or more NF zones in a room, analytically solving the linked differential equations would be decidedly more difficult than solving 2 linked differential equations, assuming that an analytical solution for the system could be found in the first place.

The $C_{WMR2}(t)$ equation by itself is convenient where the values of V and Q for the larger space are not known, or where V and Q cannot be defined because the NF zone is in ambient air outdoors. In this situation, $C_{WMR2}(t)$ provides a lower-bound estimate of exposure intensity. Given an enclosed space where β and Q are on the same order of magnitude, as in the hypothetical scenarios posed in this analysis, the $C_{WMR2}(t)$ lower-bound increases underestimation. However, in the outdoor environment where β is determined by ambient wind speeds that may be 1 to 10 mph, contaminant would rapidly disperse away from the NF zone and a lingering background concentration would be at a relatively low level. In turn, $C_{WMR2}(t)$ should be a close approximation of $C_{NF}(t)$.

Conflict of interest statement

None declared.

Funding

There was no funding support for this article and no potential conflicts of interest to declare.

Data availability

No data were used for this analysis.

Supplementary material

Supplementary material are available at *Annals of Work Exposures and Health* online.

References

American Conference of Governmental Industrial Hygienists. Industrial ventilation – a manual of recommended

practice. 23rd ed. Cincinnati: ACGIH; 1998. ISBN 1-882417-22-4

Baldwin PEJ, Maynard AD. A survey of wind speeds in indoor workplaces. Ann Occup Hyg. 1998:42(5):303–313. https://doi.org/10.1016/s0003-4878(98)00031-3.

Hemeon WCL. Plant and process ventilation. New York: The Industrial Press; 1955.

IH MOD 2.0 Version 2.016 June 2023. Available at https://www.aiha.org/public-resources/consumer-resources/apps-and-tools-resource-center/aiha-risk-assessment-tools/ihmod-tool. [accessed 2023 Jul 27].

Jayjock M, Armstrong T, Taylor M. The Daubert standard as applied to exposure assessment modeling using the two-zone (NF/FF) model estimation of indoor air breathing zone concentration as an example. J Occup Environ Hyg. 2011:8:D114–D122. https://doi.org/10.1080/15459624.2011.624387.

Keil CB, Nicas M. Predicting room vapor concentrations due to spills of organic solvents. AIHA J. 2003:64(4):445–454. https://doi.org/10.1080/15428110308984838.

Nicas M. Estimating exposure intensity in an imperfectly mixed room. Am Ind Hyg Assoc J. 1996:57(6):542–550. https://doi.org/10.1080/15428119691014756.

Nicas M. Turbulent eddy diffusion models. In: Keil CB, Simmons CE, Anthony TR, editors. Mathematical models for estimating occupational exposure to chemicals. 2nd ed. Fairfax: AIHA; 2009.

Nicas M. Mathematical modeling of indoor air contaminant concentrations. In: V Rose, B Cohrssen, editors. Patty's Industrial Hygiene, Sixth Edition, Volume 2. Hoboken, New Jersey: John Wiley & Sons. Inc.; 2011.

Nicas M. The near field/far field model with constant application of chemical mass and exponentially decreasing emission of the mass applied. J Occup Environ Hyg. 2016:13(7):519–528. https://doi.org/10.1080/15459624.2016.1148268.

Nicas M, Armstrong TW. Using a spreadsheet to compute contaminant exposure concentrations given a variable emission rate. AIHA J. 2003:64(3):368–375. https://doi.org/10.1080/15428110308984829.